Synthesis of Polycarbonate-Silica Nanocomposites from Copolymerization of CO_2 with Allyl Glycidyl Ether, Cyclohexene Oxide, and Sol-Gel

Chung-Sung Tan, Ting-Wu Kuo

Department of Chemical Engineering, National Tsing Hua University, Hsinchu, Taiwan, 30013, Republic of China

Received 26 August 2004; accepted 14 January 2005
DOI 10.1002/app.22126
Published online in Wiley InterScience (www.interscience.wiley.com).

ABSTRACT: The copolymerization of carbon dioxide, allyl glycidyl ether, and cyclohexene oxide catalyzed by the system consisting of $Y(CF_3CO_2)_3$, $Zn(Et)_2$, and pyrogallol in the solvent of 1, 3-dioxolane was performed in this study. The IR, ^1H NMR, and ^{13}C-NMR spectra, as well as the elemental analysis, indicated that the resulting copolymer was an alternating polycarbonate possessing more than 90% of carbonate units. The molecular weight could be as high as 1.5×10^5, and the polydispersity index was 4.5. The resultant polycarbonate was found to effectively react with 3-(trimethoxysilyl)propyl methacrylate via a free radical reaction to result in a precursor used in the sol-gel process to synthesize a polycarbonate-silica nanocomposite. The nanocomposites were characterized by SEM, ^{29}Si NMR, TGA, DSC, and UV–Vis. Silica particles with size less than 100 nm were found to disperse uniformly in the nanocomposites. It was also found that the thermal properties were dependent on the content of cyclohexene carbonate units. Both the thermal and mechanical properties of the resultant nanocomposites could be adjusted with silica content, while the transparency was comparable to the base copolymer even at high silica contents. © 2005 Wiley Periodicals, Inc. J Appl Polym Sci 98: 750–757, 2005

Key words: copolymerization; mechanical properties; nanocomposites; polycarbonates; thermal properties

INTRODUCTION

The reduction of greenhouse gases has been a great issue in environmental protection. It is well known that carbon dioxide (CO_2) is the major greenhouse gas; therefore, it is necessary to recycle and utilize CO_2 to cope with the reduction demand. One of the possibilities is to generate polycarbonates using carbon dioxide as the starting monomer.

Rare-earth coordination catalyst systems have proved to be effective for synthesis of polycarbonates from CO_2 and aliphatic epoxides.[1–3] However, the generated copolymers have their limitations on thermal and mechanical properties. These properties may be improved using both a cyclic epoxide and an aliphatic epoxide as the starting monomers in copolymerization.[4] But brittleness and lack of transparency are the major drawbacks of the resulting block copolymers. Recently, the sol-gel process coupled with polymerization to generate polymer-inorganic hybrid material has attracted much attention in material synthesis.[5–8] The major advantage of a sol-gel process is its low temperature and pressure operation. Besides, the thermal and mechanical properties can be easily manipulated by interaction between the dispersed and continuous phases. Due to the nano-scale of the dispersed inorganic particles, the transparency can be maintained as high as that of the parent polymer. Tan and coworkers[9] have successfully combined copolymerization of CO_2 with allyl glycidyl ether (AGE) with a sol-gel process to generate a polycarbonate-silica nanocomposite in which the thermal and mechanical properties are well improved as compared to the polycarbonate itself.

In this study the copolymerization of CO_2, AGE, and cyclohexene oxide (CHO) using an yttrium-metal coordination catalyst was carried out to synthesize poly(AGE-CHO carbonate) (PACC). The most appropriate temperature in the synthesis was determined through the yield and molecular weight of PACC. The nanocomposite precursors possessing a trimethoxysilyl functional group were then prepared by a free radical reaction of PACC with 3-(trimethoxysilyl)propyl methacrylate (MSMA) using benzoyl peroxide (BPO) as the initiator. The PACC-SiO_2 nanocomposite was then generated by a sol-gel process in which tetraethoxysilane (TEOS) was used in the presence of the catalyst HCl. The thermal and mechanical properties of PACC-SiO_2 nanocomposites were measured and compared to those of the PACC base material.

EXPERIMENTAL

AGE with a purity of 99% (Tokyo Chemical Industry), CHO with a purity of 98% (Tokyo Chemical Industry), and propylene oxide (PO) with a purity of 99.5%

Correspondence to: C.-S. Tan (cstan@che.nthu.edu.tw).

TABLE I
Yield and Molecular Weight of the PACC Synthesized at Conditions: $Y(CF_3CO_2)_3$ = 0.0004 mol; $Zn(Et)_2$ = 0.004 mol; pyrogallol = 0.008 mol; solvent = 1,3-dioxolane of 30 ml; P = 2.76 MPa; time = 12 h

T (K)	Yield (g/g of Zn)	$M_w \times 10^{-5}$	M_w/M_n	T_g (K)	T_{10} (K)	f_{CO_2} (%)	f_{AGC} (%)	f_{CHC} (%)
333	57	1.6	4.48	329	587	63.4	17.6	45.8
343	63	1.5	4.44	327	587	66.1	19.5	46.6
353	71	1.5	4.54	336	580	93.0	28.0	65.0

(Janssen Chimica) were refluxed over CaH_2 for 4 h and then distilled before use. Diethyl zinc $Zn(Et)_2$, TEOS, MSMA, HCl, and all the solvents, including 1,3-dioxolane, methanol, tetrahydrofuran (THF), and *n*-hexane, were of analytical reagent grade and were used without further treatment. Carbon dioxide of a purity of 99.99% (Air Product) was used as received. Yttrium trifluoroacetate $Y(CF_3CO_2)_3$ and pyrogallol were heated in vacuum at 353 K for 40 h, and BPO was recrystallized from acetone before use.

The rare-earth coordination catalyst system composed of $Y(CF_3CO_2)_3$, $Zn(Et)_2$, and pyrogallol was prepared in an atmosphere of argon. The preparation was done by first dissolving pyrogallol in a solvent, such as 1,3-dioxolane. The resultant solution was then added dropwise to the solution of $Zn(Et)_2$ and the same solvent at room temperature. The solution containing suspended powders was heated at 333 K for 2 h, and was then added to a 300 mL autoclave equipped with a magnetic stirrer (Autoclave Engineers Inc.) in which a known amount of $Y(CF_3CO_2)_3$ was present. Before the addition of the solution, the autoclave was heated in vacuum at 373 K for 4 h to remove oxygen and moisture. The resultant rare-earth catalyst solution was stirred at 333 K for 1 h before CO_2 and epoxides were introduced.

The copolymerization proceeded in the autoclave loaded with the prepared catalyst system at a spinning speed of 1000 rpm after introducing CO_2, AGE, and CHO. After a 12 h reaction period, the pressure was reduced to atmosphere to terminate the copolymerization, and an excess of aqueous methanol solution containing 10 wt % HCl was added to the result in the precipitation of the crude copolymer. The precipitated copolymer was purified by dissolving it in THF first and then adding an aqueous methanol solution (50 wt %) to precipitate the copolymer again. After three times of purification, the copolymer PACC was dried under vacuum at 313 K for 8 h prior to analysis and further use.

To prepare the precursor used in the sol-gel process, the generated PACC was reacted with MSMA via a free radical reaction using BPO as the initiator at 353 K. In the preparation, 3.0 g of PACC, MSMA, and BPO (1.0 mol % of MSMA) were dissolved in THF to result in a concentration of 2.5 wt %. The resultant copolymer precursor was purified by reprecipitation in *n*-hexane. After three times of purification, the precursor was dried under vacuum at 313 K for 4 h.

The PACC-SiO_2 nanocomposites were synthesized via a sol-gel process. In the synthesis, a solution denoted as Sol-A was prepared by dissolving the copoly-

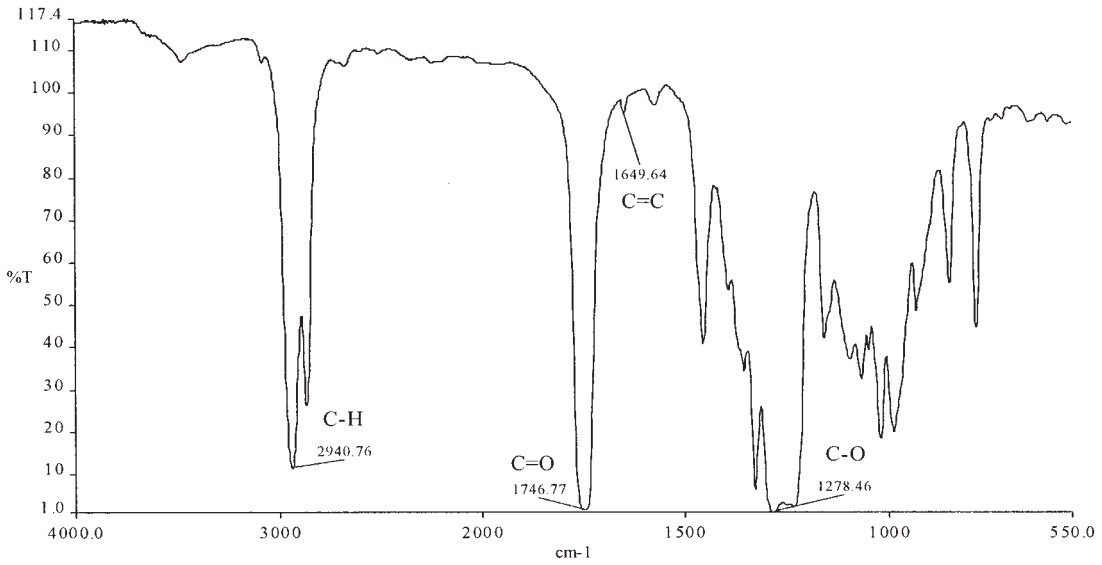

Figure 1 The IR spectrum of the resultant PACC at the copolymerization conditions: $Y(CF_3CO_2)$ = 0.0004 mol; $Zn(Et)_2$ = 0.004 mol; pyrogallol = 0.008 mol; solvent = 1,3-dioxolane of 30 ml; T = 353 K; P = 2.76 MPa; time = 12 h.

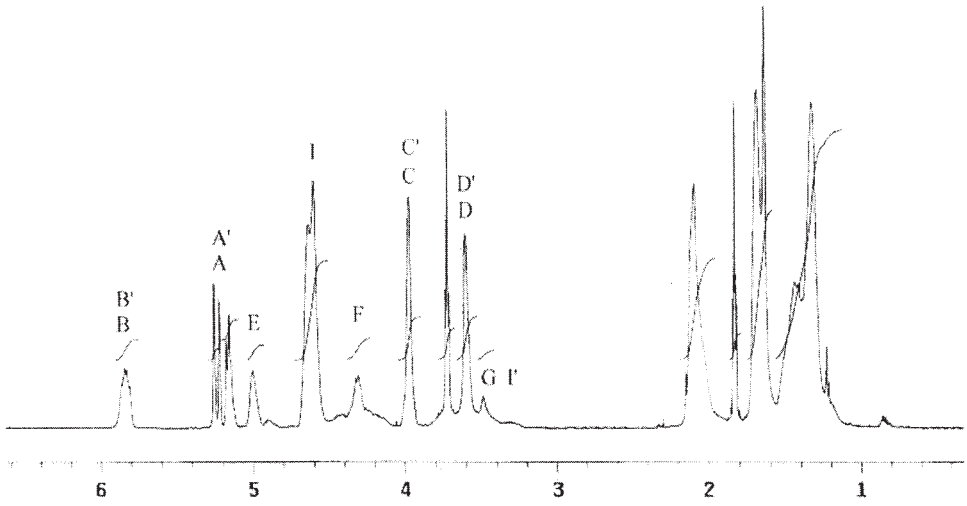

Figure 2 The ^{1}H NMR spectrum of the resultant PACC at the copolymerization conditions: $Y(CF_3CO_2)$ = 0.0004 mol; $Zn(Et)_2$ = 0.004 mol; pyrogallol = 0.008 mol; solvent = 1,3-dioxolane of 30 ml; T = 353 K; P = 2.76 MPa; time = 12 h.

mer precursor in THF, and another solution denoted as Sol-B was prepared by mixing THF, TEOS, and HCl. The Sol A and Sol B were mixed in a beaker under vigorous stirring for 10 min to result in a clear homogenous solution. After vaporization of H_2O and methanol resulting from hydrolysis and condensation in the sol-gel process as well as the solvent THF, a clear gel was formed. The formed gel was then cast onto a Teflon-coated plate. After drying the plate for 8 days at 303 K, a transparent film of the PACC-SiO_2 nanocomposite was generated.

The IR spectra were obtained by the Perkin–Elmer Paragon 500 spectrometer. The ^{1}H NMR and ^{13}C NMR spectra were recorded with a Varian spectrometer (Uniytinova-500, 500 and 125 MHz) using *d*-chloroform as the solvent. The glass transition temperatures (T_g) of PACC and PACC-SiO_2 were measured by a DSC (Dupont 951) with a heating rate of 5 K/min. The thermal degradation of PACC and PACC-SiO_2 was measured by a TGA (Dupont 951) with a heating rate of 20 K/min from room temperature to 1073 K.

The molecular weight and polydispersity indexes were determined by a gel permeation chromatograph (Shimadzu LC-9A) using THF as the solvent and polystyrene as the standard. The elemental analysis was carried out in the Perkin–Elmer CHN 2400. The silicon content was calculated by heating PACC and PACC-SiO_2 in a Muffle Furnace DF 20 SJ

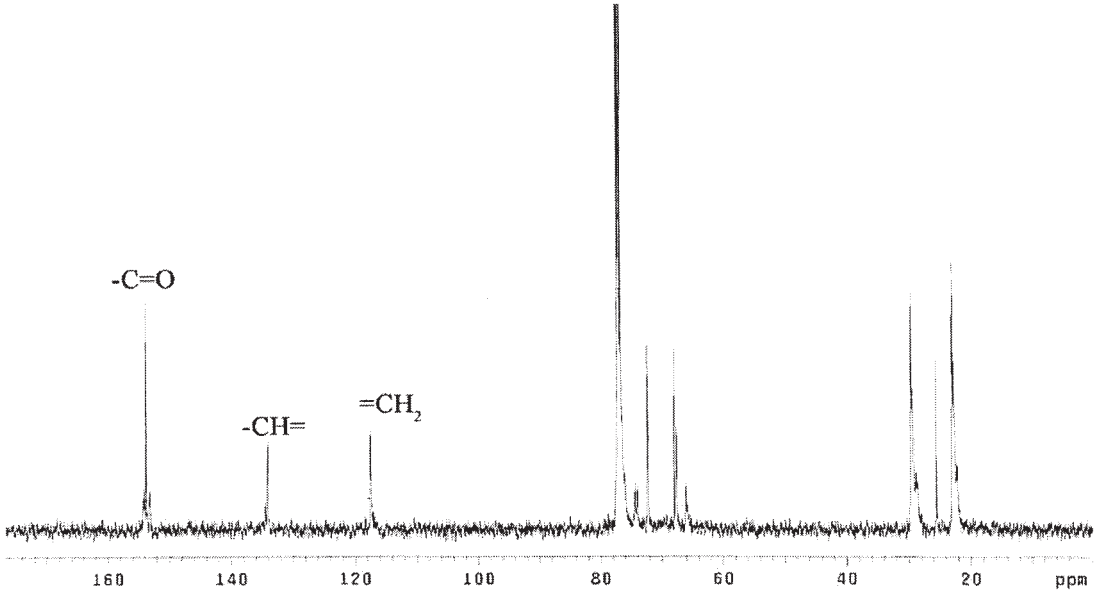

Figure 3 The ^{13}C NMR spectrum of the resultant PACC at the copolymerization conditions: $Y(CF_3CO_2)$ = 0.0004 mol; $Zn(Et)_2$ = 0.004 mol; pyrogallol = 0.008 mol; solvent = 1,3-dioxolane of 30 ml; T = 353 K; P = 2.76 MPa; time = 12 h.

TABLE II
Si Contents in Precursors Generated using BPO as the Initiator

PACC[a]	MSMA, g	THF, g	Time, h	Si, %
3.00 g	0.63	116.4	10	0.00
3.00 g	1.26	115.7	10	0.27
3.00 g	3.78	113.2	10	1.10
3.00 g	6.30	110.6	10	1.35

[a]Synthesis conditions: $Y(CF_3CO_2)_3$ = 0.0004 mol; $Zn(Et)_2$ = 0.004 mol; pyrogallol = 0.008 mol; solvent = 1,3-dioxolane of 30 ml; T = 353 K; P = 2.76 MPa; time = 12 h.

at 1273 K. The structure of PACC-SiO_2 was identified by ^{29}Si NMR (Bruker DSX-400WB). The mechanical properties, such as tensile strength, tensile modulus, and elongation at break, of PACC and PACC-SiO_2 were measured in accordance with ASTM test method D-368 (Instron Mini 44). The morphology of the fractured surface of PACC-SiO_2 was observed by SEM and Si-mapping photographs (Hitachi S-4700). The transparency was measured by a UV–Vis spectrometer (Hitachi U-3300).

RESULTS AND DISCUSSION

Characterization of PACC

As indicated by Hsu and Tan[10] and Tan and colleagues,[9] the most appropriate pressure for both the copolymerization of CO_2 with CHO and CO_2 with AGE was at 2.76 MPa, and the most appropriate temperatures are at 353 K and 333 K, respectively. The pressure for the copolymerization of CO_2 with AGE and CHO was therefore maintained at 2.76 MPa, and the temperature was varied from 333 to 353 K for the coordination catalyst system consisting of $Y(CF_3CO_2)_3$, $Zn(Et)_2$, and pyrogallol. Table I shows the copolymerization at 353 K resulted in the highest yield and carbonate content (f_{CO2}); subsequently, the copolymer was therefore synthesized at this temperature. The resultant copolymer is supposed to possess the following chemical structure:

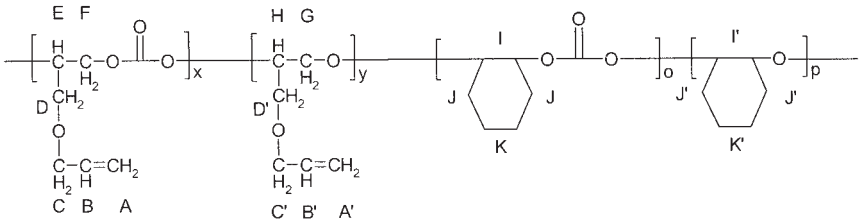

The two absorption peaks at ~ 1250 and 1750 cm^{-1} in the IR spectra shown in Figure 1 indicate the presence of carbonate units in the resultant copolymer. There also exists an absorption peak at ~ 1650 cm^{-1}, indicating the presence of C═C double bonds. Figures 2 and 3 are the ^{1}H NMR and ^{13}C NMR spectra of the resultant copolymer, respectively. By comparing the spectra with that for the copolymerization of CO_2 with AGE[9] and CO_2 with CHO,[10] it is concluded that the resultant copolymer was an alternating polycarbonate containing AGE and CHO carbonate units. In the ^{1}H NMR spectra, the area of the absorption peak of AGE and CHO ethers denoted as $A_{3.5\sim3.8}$, the area of the absorption peak of allyl glycidyl carbonate (AGC) denoted as $A_{4.0}$, and the area of the absorption peak of cyclohexene carbonate (CHC) denoted as $A_{4.6}$ can be determined. Based on the following equations, the carbonate unit content (f_{CO2}), allyl glycidyl carbonate content (f_{AGC}), and cyclohexene carbonate content (f_{CHC}) can then be calculated:

$$f_{CO_2} = 1 - \left(\frac{A_{3.5\sim3.8}}{A_{3.5\sim3.8} + A_{4.0} + A_{4.6}}\right) \quad (1)$$

$$f_{AGC} = \left(\frac{A_{4.0}}{A_{3.5\sim3.8} + A_{4.0} + A_{4.6}}\right) \quad (2)$$

$$f_{CHC} = \left(\frac{A_{4.6}}{A_{3.5\sim3.8} + A_{4.0} + A_{4.6}}\right) \quad (3)$$

Table I indicates that the carbonate units, f_{AGC} and f_{CHC}, of the generated PACC varied at different temperatures. When the reaction temperature was raised from 333 to 353 K, more ring-opening of CHO and insertion of CO_2 occurred to form a cyclohexene carbonate unit. Besides, the rigid cyclohexene carbonate could stabilize the allyl glycidyl carbonate unit and therefore prevent AGE from cracking under high temperatures. As a result, both carbonate units were increased with increasing temperature. The contents of carbonate units evaluated from the ^{1}H NMR spectra were also checked by elemental analysis. The differences in C and H contents evaluated by the ^{1}H NMR spectra and elemental analysis were found to be 0.3% and 3.0%, respectively, indicating the accuracy of the evaluated carbonate unit contents from the ^{1}H NMR spectra.

In the free radical reaction of PACC with MSMA, the amount of the initiator BPO was increased with the increasing amount of MSMA added to maintain a constant molar ratio of MSMA to BPO. The resultant sol-gel precursor is supposed to have the following chemical structure:

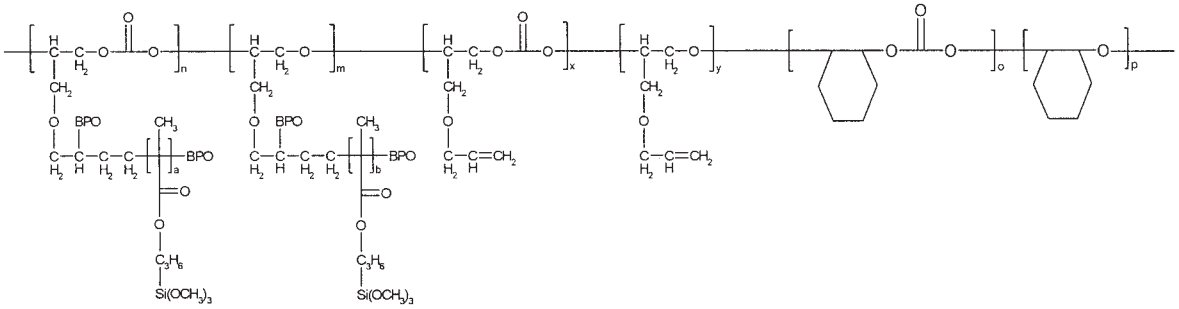

It is seen from Table II that the Si content in PACC was zero when only a small amount of MSMA was added, indicating that the amount of the initiator was not high enough to proceed the free radical reaction. When both BPO and MSMA were increased, the Si content in the resulting precursor was found to increase, as shown in Table II. But when more BPO was added, the vinyl group in PACC became more active to react with itself. As a result, gelation was observed to happen for the case that 6.3 g of MSMA was added. In this situation, the Si content of 1.1% in the resulting precursor was chosen for the subsequent sol-gel process. Figure 4 shows the presence of the absorption peak of $-OCH_3$ in the ^{13}C NMR spectrum at the Si content of 1.1%, indicating that PACC was functionalized via the free radical reaction.

Characterization of PACC-SiO_2 nanocomposite

Figures 5 and 6 are the SEM and Si-mapping photographs of the fractured surfaces of the PACC-SiO_2 nanocomposites resulting from the addition of TEOS into the functionalized precursor in the sol-gel process. The photographs show that the SiO_2 particles were dispersed uniformly in the generated nanocomposite. The size of the SiO_2 domains was generally enlarged with increasing the added amount of TEOS. All the sizes were found to be less than 100 nm when the Si content was less than 7%. Agglomeration occurred at high Si contents, but was not so severe.

Figure 7 shows the ^{29}Si NMR spectra of the precursor and PACC-SiO_2 nanocomposites. As expected, only the type of Si atom at about -48 ppm equivalent to the T^1 structure existed in the precursor.[11] For the

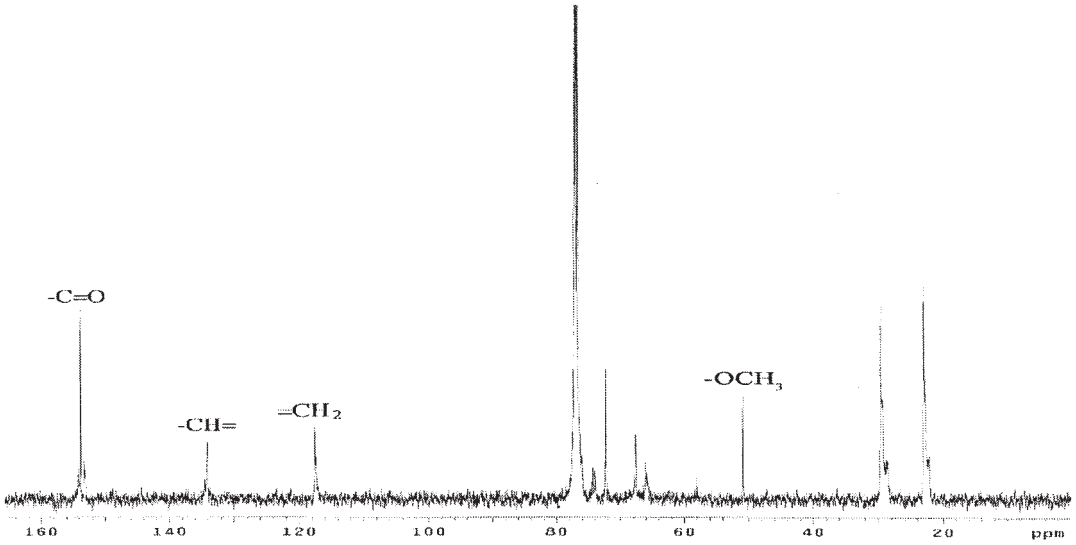

Figure 4 The ^{13}C NMR spectrum of the functionalized PACC with the silicon content of 1.1%.

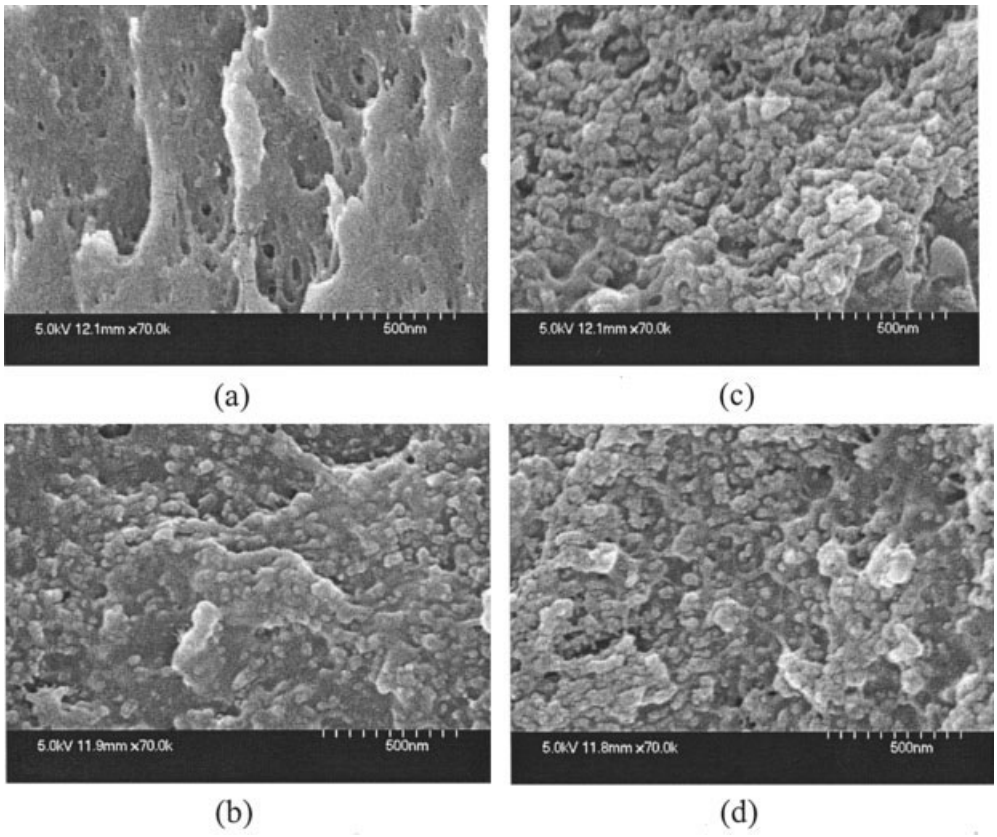

Figure 5 The SEM photographs of the PACC-SiO_2 nanocomposites with different Si contents: (a) 3.6%, (b) 7.0%, (c) 9.0%, and (d) 11.5%.

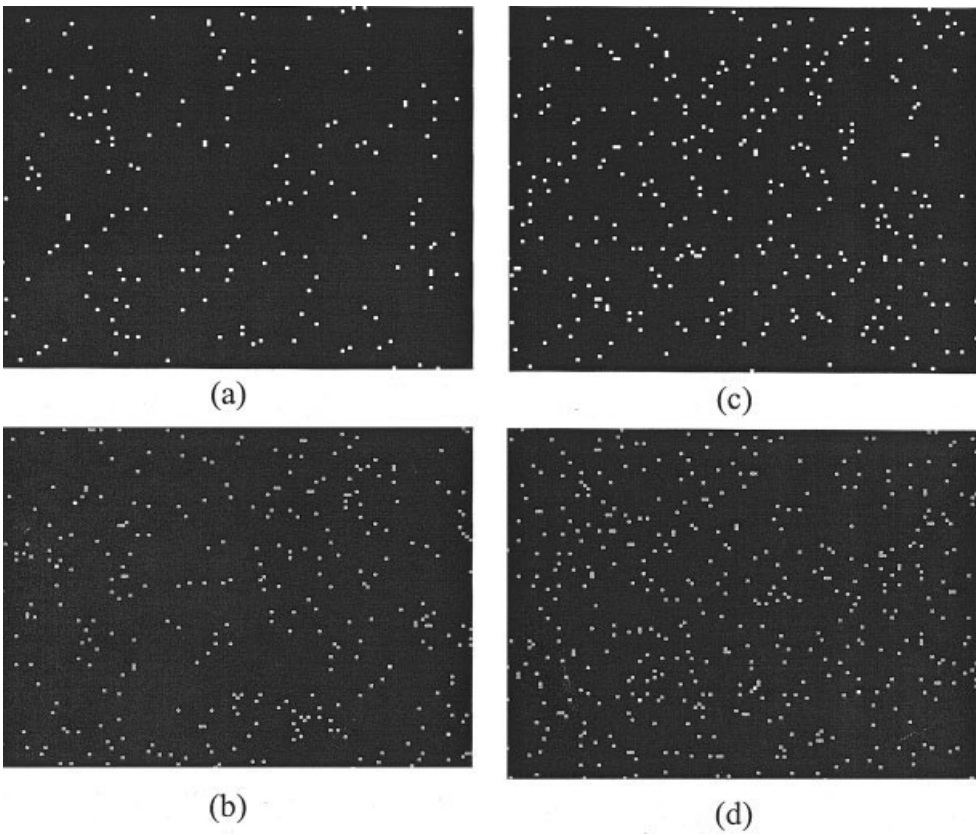

Figure 6 The Si-mapping photographs of the PACC-SiO_2 nanocomposites with different Si contents: (a) 3.6%, (b) 7.0%, (c) 9.0%, and (d) 11.5%.

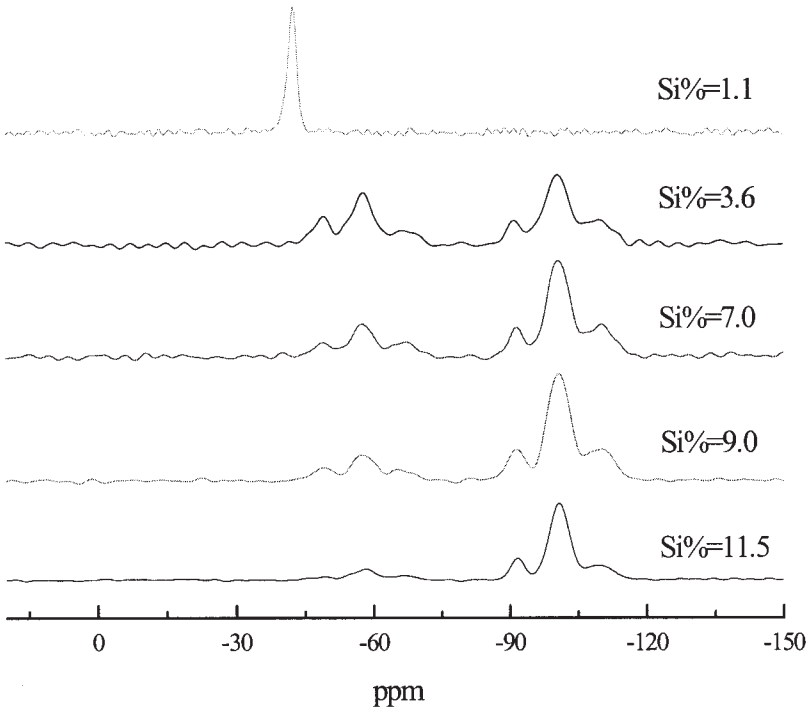

Figure 7 The ^{29}Si NMR spectra of the precursor and the PACC-SiO_2 nanocomposites.

PACC-SiO_2 nanocomposites, there existed three types of silicon atom, Q^2, Q^3, and Q^4 structures, at -90, -100, and -110 ppm, respectively, indicating the formation of a silica network.[9,11] It is also seen from Figure 7 that when the Si content was increased, the T^1 structure was split into T^1, T^2, and T^3, and the total areas of T^n ($n = 1 \sim 3$) structures decreased, indicating the presence of a chemical bonding between the organic and inorganic phases.

Mechanical and thermal properties of nanocomposites

Table III presents the mechanical properties of the PACC-SiO_2 nanocomposites. When the Si content was increased, the tensile strength and the tensile modulus were both increased. With the introduction of SiO_2 into PACC, the elongation at break decreased with an increase in Si content. The transparency of the resultant PACC-SiO_2 nanocomposites was found to maintain a value within 95% of the base PACC no matter at what Si contents, providing evidence that the silica particles were in nano-scale and the distribution of the particles was rather uniform in the nanocomposites.

Table IV shows the thermal properties of the PACC-SiO_2 nanocomposites with f_{AGC} of 28% and f_{CHC} of 65%. When the Si content was increased, both the glass transition temperature (T_g) and the thermal degradation temperature (T_{10}) were found to decrease. The decrease in T_g and T_{10} was also observed in the organic-inorganic hybrids containing higher fractions of more rigid chemical structures, such as cyclic rings.[12,13] Due to the presence of a high fraction of the rigid structure CHC in the nanocomposites, the steric hindrance on the formation of a silica network was believed to be pronounced. As a consequence, T_g and T_{10} were lowered as compared to the parent copolymer. With this consideration, it is therefore expected that the thermal behavior would be different for the nanocomposites with different fractions of CHC and AGC. A PACC with f_{AGC} of 40% and f_{CHC} of 55% generated by changing the monomer feedings in the copolymerization was synthesized. It was used as the base copolymer to

TABLE III
The Mechanical Properties of the PACC-SiO_2 Nanocomposites with Different Si Contents (PACC was with f_{AGC} of 28% and f_{CHC} of 65%)

Si, %	0.0	3.6	7.0	9.0	11.5
Tensile strength (MPa)	11.9 ± 0.6	14.9 ± 0.7	15.1 ± 0.8	15.5 ± 0.8	16.2 ± 0.8
Tensile modulus (MPa)	246.7 ± 12.3	270.3 ± 13.5	328.6 ± 16.4	340.3 ± 17.0	379.6 ± 19.0
Elongation at break (%)	25 ± 1.3	16 ± 0.8	13 ± 0.7	7 ± 0.4	2 ± 0.1

TABLE IV
The Thermal Properties of the PACC-SiO_2 Nanocomposites with Different Si contents (PACC was with f_{AGC} of 28% and f_{CHC} of 65%)

Si %	0	1.1	3.6	7.0	9.0	11.5
T_g (K)	336	332	332	329	328	328
T_{10} (K)	580	572	573	578	574	569

generate the nanocomposite following the above-mentioned preparation steps. Table V shows that T_g and T_{10} were all increased with increasing Si content.

Not only PACC, but a copolymer denoted as PAPC resulting from the copolymerization of CO_2 with AGE and PO was synthesized as well. No rigid chemical structures were present in this kind of copolymer. From the measured ^1H NMR spectra, the copolymer was found to contain AGE carbonate and PO carbonate of 24 and 76%, respectively. With the same preparation steps as for the PACC-SiO_2 nanocomposite, the nanocomposite consisting of PAPC and SiO_2 was generated. Table VI shows the expectation that the thermal properties were all enhanced with an increase in Si content.

CONCLUSIONS

An alternating polycarbonate PACC could be effectively synthesized from the copolymerization of CO_2, AGE, and CHO at 353 K and 2.76 MPa using the coordination catalyst system composed of $Y(CF_3COO)_3$-$Zn(Et)_2$-pyrogallol and the solvent 1,3-dioxolane. The molecular weight and its distribution, as well as the carbonate fraction including allyl glycidyl carbonate and cyclohexene carbonate, of the resultant PACC were found to be 1.5×10^5, 4.54, and more than 90%, respectively.

TABLE V
The Thermal Properties of the PACC-SiO_2 Nanocomposites with Different Si Contents (PACC was with f_{AGC} of 40% and f_{CHC} of 55%)

Si %	0	1.1	3.2	7.0	9.0	11.2
T_g (K)	315	314	317	320	323	325
T_{10} (K)	566	562	573	580	582	584

TABLE VI
The Thermal Properties of the PAPC-SiO_2 Nanocomposites with Different Si Contents

Si %	0	0.96	4.0	7.0	8.3	10.6
T_g (K)	297	296	303	306	307	310
T_{10} (K)	529	533	543	543	552	553

The functionalized PACC containing the structure $-OCH_3$ used as the precursor in the synthesis of the PACC-SiO_2 nanocomposite was generated successfully via a free radical reaction with MSMA using BPO as the initiator. The most appropriate Si content in the precursor was found to be 1.1%. The PACC-SiO_2 nanocomposites were then successfully synthesized through a sol-gel process in which TEOS was used as the silica precursor. From the SEM and Si-mapping photographs of the fractured surfaces of PACC-SiO_2, it was confirmed that nano-scale SiO_2 particles could be dispersed uniformly in the resultant nanocomposites. With the addition of nano SiO_2 particles, the glass transition and thermal degradation temperatures were found to be dependent on the structure of the nanocomposites. Both the mechanical and thermal properties could be adjusted with Si content, while the transparency could still be maintained compared to the base PACC.

Financial support from the National Science Council of ROC (Grant NSC93–2214-E-007–009) is gratefully acknowledged.

References

1. Chen, X.; Shen, Z.; Zhang, Y. Macromolecules 1991, 24, 5305.
2. Hsu, T. J.; Tan, C. S. Macromolecules 1997, 30, 3147.
3. Liu, B.; Zhao, X.; Wang, X.; Wang, F. Polymer 2003, 44, 1803.
4. Hsu, T. J.; Tan, C. S. Polymer 2002, 43, 4535.
5. Wei, Y.; Bakthavatchalam, R.; Yang, D.; Whitecar, C. K. Polym Prepr 1991, 32, 503.
6. Wen, J.; Wilkes, G. L. Chem Mater 1996, 8, 1667.
7. Schottner, G. Chem Mater 2001, 13, 3422.
8. Kim, J. W.; Cho, W. J.; Ha, C. S. J Polym Sci Polym Phys 2002, 40, 19.
9. Tan, C. S.; Juan, C. C.; Kuo, T. W. Polymer 2004, 45, 1805.
10. Hsu, T. J.; Tan, C. S. Polymer 2001, 42, 5143.
11. Joseph, R.; Zhang, S.; Ford, W. T. Macromolecules 1996, 29, 1305.
12. Wei, Y.; Yang, D.; Tang, L. J Mater Res 1993, 8, 5.
13. Chen, Y.; Iroh, J. O. Chem Mater 1999, 11, 1218.